Perspectives of Silicon for Future Spintronic Applications From the Peculiarities of the Subband Structure in Thin Films

Oskar Baumgartner, Viktor Sverdlov, Thomas Windbacher, and Siegfried Selberherr, *Fellow, IEEE*

***Abstract*—The two-band k·p model for the conduction band is used to analyze the subband structure in (0 0 1) thin silicon films. In contrast to the usually assumed parabolic energy dispersion, the two-band k·p model is able to describe the conduction band structure in the presence of shear strain. It is demonstrated that the unprimed subbands are degenerate only in relatively thick relaxed films. In thin films, the subbands develop different in-plane effective masses. In orthogonal magnetic fields, this leads to a subband splitting linear in the field strength. It also results in a large subband splitting that is observed in [1 1 0]-oriented point contacts. With shear strain, the degeneracy between the unprimed subbands in (0 0 1) films is lifted. This splitting depends strongly on the film thickness and becomes large in ultrathin films. Strain-induced valley splitting results in reduced scattering and increased spin coherent time, which makes silicon attractive for future spintronic applications.**

***Index Terms*—Shear strain, two-band k·p model, valley splitting.**

I. Introduction

THE RAPID increase in computational power and speed of integrated circuits is supported by the incessant reduction of semiconductor devices' feature size. Due to constantly introduced innovative changes in the technological processes, the miniaturization of MOSFETs institutionalized by Moore's law successfully continues. The 32-nm MOSFET process technology by Intel [1], [2] involves new high-k dielectric/metal gates, which represents a major change in the technological process since the invention of MOSFETs. Although alternative channel materials with a mobility higher than in Si were already investigated [3], [4], it is believed that Si will still be the main channel material for MOSFETs beyond the 22-nm technology node.

With scaling apparently approaching its fundamental limits, the semiconductor industry is facing critical challenges. New engineering solutions and innovative techniques are required to improve CMOS device performance. Strain-induced mobility enhancement is one of the most attractive solutions to increase the device speed, which will certainly maintain its key position among possible technological innovations for future technology generations. In addition, new device architectures based on multigate structures with better electrostatic channel control and reduced short channel effects will be developed. A multigate MOSFET architecture is expected to be introduced for the 16-nm technology node. Combined with a high-k dielectric/metal gate technology and strain engineering, a multigate MOSFET appears to be the ultimate device for high-speed operation with excellent channel control, reduced leakage currents, and low-power budget. Confining carriers within a thin film reduces the channel dimension in transversal direction, which further improves gate channel control.

At the same time, the search for post-CMOS device concepts has accelerated. A quantum computer promises to open new horizons to approach large-scale computations. Quantum mechanical properties in representing the data should lead to a substantial superiority in quantum computation over classical approaches. Although the concept is very attractive, quantum calculations in experiment were performed on a small number of qubits only. There are several extremely challenging problems that prevent the building of a large quantum computer, and more research is needed. One particular problem is how to maintain the quantum state coherence within qubits.

Spin as a degree of freedom is promising for future nanoelectronic devices and applications. A concept of a racetrack memory recently proposed in [5] is based on the controlled domain wall movement by spin-polarized current in magnetic nanowires. Silicon, the main element of microelectronics, possesses several properties attractive for spintronic applications. Silicon is composed of nuclei with predominantly zero spin and is characterized by small spin-orbit coupling. In a recent ground-breaking experiment coherent spin transport through an undoped silicon wafer of 350 μm length was demonstrated [6]. The experiment was possible due to a unique injection and detection technique of polarized spins delivered through thin ferromagnetic films. Coherent propagation of spins at such long distances makes the fabrication of spin-based switching devices likely already in the near future.

Spin-controlled qubits may be thought of as a basis for upcoming logic gates. However, the conduction band of silicon contains six equivalent valleys, which is a source of potentially increased decoherence. For successful applications, the

Manuscript received June 12, 2009; accepted August 11, 2010. Date of publication September 9, 2010; date of current version July 8, 2011. This work was supported by the Austrian Science Fund FWF under Project P19997-N14 and by the European Research Council under Grant #247056 MOSILSPIN. This paper was presented at the Silicon Nanoelectronics Workshop, Kyoto, Japan, June 13–14, 2009. The review of this paper was arranged by Associate Editor E. Wang.

The authors are with the Institute for Microelectronics, Technische Universität Wien, A-1040 Wien, Austria (e-mail: baumgartner@iue.tuwien.ac.at; sverdlov@iue.tuwien.ac.at; windbacher@iue.tuwien.ac.at; selberherr@iue.tuwien.ac.at).

Color versions of one or more of the figures in this paper are available online at http://ieeexplore.ieee.org.

Digital Object Identifier 10.1109/TNANO.2010.2074211

degeneracy between the valleys must be removed and become larger than the spin Zeeman splitting. Shubnikov-de-Haas measurements in an electron system, which is composed of thin silicon films in Si–SiGe heterostructures, reveal that the valley splitting is small [7]. At the same time, recent experiments on the conductivity measurements of point contacts created by confining a quasi-2-D electron system in lateral direction with the help of additional gates deposited on the top of the silicon film demonstrate a splitting between equivalent valleys larger than the spin splitting [7].

In this paper, we demonstrate that a large valley splitting in the confined electron system can be induced by a shear strain component. Our analysis is based on the two-band $\mathbf{k}\cdot\mathbf{p}$ model for the conduction band in silicon. The parabolic band approximation usually employed for subband structure calculations of confined electrons in Si inversion layers is insufficient in ultrathin Si films. The two-band $\mathbf{k}\cdot\mathbf{p}$ model includes strain and is shown to be accurate up to energies of 0.5 eV. This model can therefore be used to describe the subband structure in thin silicon films, where the subband quantization energy may reach a hundred millielectronvolts.

We first describe the subband structure in a thin unstrained (0 0 1) silicon film. We demonstrate that the peculiarities of the subband dispersion obtained within the two-band $\mathbf{k}\cdot\mathbf{p}$ model result in a linear dependence of the valley splitting on the magnetic field. We show that a large valley splitting is observed in experiments on conduction quantization through a quantum point contact in [1 1 0] direction, but the splitting is suppressed in [1 0 0] point contacts. Finally, we demonstrate that the valley splitting is considerably enhanced in films strained in [1 1 0] direction.

II. Two-Band $\mathbf{k}\cdot\mathbf{p}$ Model

The closest band to the lowest conduction band Δ_1 near its minimum is the second conduction band Δ_2. These two bands are degenerating exactly at the X point. Since the minimum of the lowest conduction band in unstrained silicon is only $k_0 = 0.15(2\pi)/a$ away from the X point, where a is the lattice constant of unstrained silicon, the two bands must be included on equal footing in order to describe the dispersion around the minimum. More distant bands separated by larger gaps are included in the second-order $\mathbf{k}\cdot\mathbf{p}$ perturbation theory [8], which results in the following two-band $\mathbf{k}\cdot\mathbf{p}$ Hamiltonian [9]:

$$H = \left(\frac{\hbar^2 k_z^2}{2m_l} + \frac{\hbar^2(k_x^2+k_y^2)}{2m_t}\right) I + \left(D\varepsilon_{xy} - \frac{\hbar^2 k_x k_y}{M}\right)\sigma_x + \frac{\hbar^2 k_z k_0}{m_l}\sigma_z \quad (1)$$

where $\sigma_{x,z}$ are the Pauli matrices, I is the 2×2 unity matrix, m_t and m_l are the transversal and the longitudinal effective masses, respectively, ε_{xy} denotes the shear strain component, $M^{-1} \approx m_t^{-1} - m_0^{-1}$, and $D = 14$ eV is the shear strain deformation potential [9], [10]. This is the only form of the Hamiltonian in the vicinity of the X point allowed by symmetry considerations [8]. The two-band Hamiltonian (1) results in the following dispersion relations:

$$E = \frac{\hbar^2 k_z^2}{2m_l} + \frac{\hbar^2(k_x^2+k_y^2)}{2m_t} \pm \sqrt{\left(\frac{\hbar^2 k_z k_0}{m_l}\right)^2 + \delta^2} \quad (2)$$

where the negative sign corresponds to the lowest conduction band,

$$\delta^2 = (D\varepsilon_{xy} - \hbar^2 k_x k_y / M)^2.$$

The energy E and k_z are counted from the X point. A comparison of (2) with the band structure of [0 0 1] valleys obtained numerically with the density functional theory (DFT) [11]–[14], the empirical pseudopotential method (EPM) [10], and with the tight-binding sp^3d^5 s^* model [15] in [1 0 0] and [1 1 0] directions is shown in Fig. 1. The empirical tight-binding sp^3d^5 s^* model with parameters from [15] seems to underestimate the anisotropy of the conduction band. The reason for such a behavior is displayed in Fig. 2. The minimum of the conduction band within the tight-binding model is located further away from the X point than k_0. This leads to a gap between the two bands at the minimum of the lowest conduction band, which is nearly two times larger than the corresponding gap from EPM calculations. Since the warping of the conduction band is determined by the band interaction, the larger gap results in less coupling and a lower degree of anisotropy.

The $\mathbf{k}\cdot\mathbf{p}$ model accurately describes the dispersion relation up to energies of about 0.5 eV. It also reproduces correctly the conduction band dispersion subject to shear strain [16]. Therefore, the $\mathbf{k}\cdot\mathbf{p}$ Hamiltonian (1) can be used to describe the subband structure in thin silicon films and inversion layers.

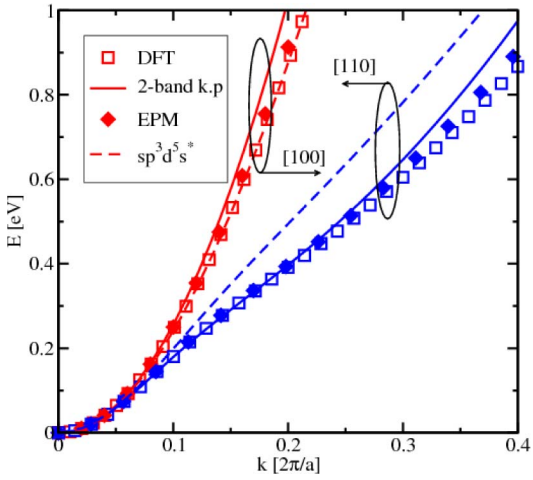

Fig. 1. Comparison of the conduction band of silicon computed with the DFT [10], the empirical EPM [9], the sp^3d^5 s^* tight-binding method [11], and the two-band $\mathbf{k}\cdot\mathbf{p}$ model [8]. The two-band $\mathbf{k}\cdot\mathbf{p}$ model is accurate up to an energy of 0.5 eV.

III. Subband Dispersion in a (0 0 1) Silicon Film: Analytical Results

A. General Equations

For [0 0 1] silicon films, the confinement potential gives an additional contribution $U(z)I$ to the Hamiltonian (1). In the

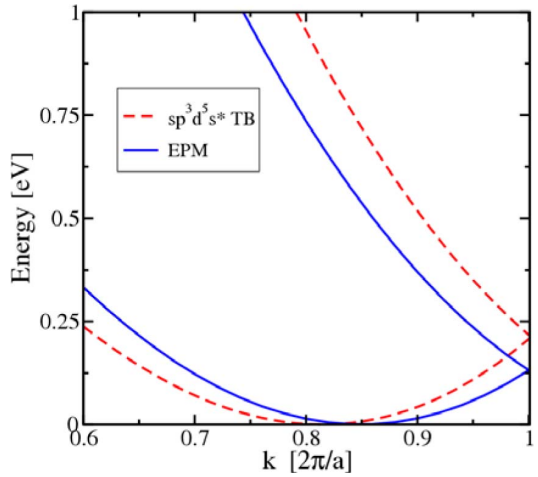

Fig. 2. Conduction band dispersion along the $\Gamma - X$-direction obtained with the EPM and the TB methods. Because of the minimum position found further away from the X point, the gap between the two conduction bands at the minimum obtained with the TB method [15] is two times larger.

effective-mass approximation described by (1) with the coefficient in front of σ_x set to zero, the confining potential $U(z)$ is known to quantize the six equivalent valleys of the conduction band of bulk silicon into the fourfold degenerate primed and the twofold degenerate unprimed subband ladder. In ultrathin films, the unprimed ladder is predominantly occupied and must be considered. The term with σ_x in (1) couples the two lowest conduction bands and lifts the twofold degeneracy of the unprimed subband ladder. The additional unprimed subband splitting, or the valley splitting, can be extracted from the Shubnikov-de-Haas oscillations and is typically in the order of a few tens microelectronvolts [7]. However, the valley splitting is significantly enhanced in a laterally confined 2-D electron gas [7]. The valley splitting is usually addressed by introducing a phenomenological intervalley coupling constant at the silicon interface [17]. Here, we investigate the valley splitting based on the two-band $\mathbf{k}\cdot\mathbf{p}$ model (1) without introducing any additional parameters.

We approximate the confining potential of an ultrathin silicon film by a square-well potential with infinite potential walls. This is sufficient for the purpose to analyze the valley splitting in a quasi-2-D gas due to interband coupling. The generalization to include a self-consistent potential is straightforward though numerically involved [18]. Because of the two-band Hamiltonian, the wave function Ψ is a spinor with the two components $|0\rangle$ and $|1\rangle$. For a wave function with space dependence in a form $\exp(ik_z z)$, the coefficients A_0 and A_1 of the spinor components are related via the equation $H\Psi = E(k_z)\Psi$. For a particular energy E, there exist four solutions k_i $(i = 1, \ldots, 4)$ for k_z of the dispersion relation (2); therefore, the spatial dependence of a spinor component α is in the form $\sum_{i=1}^{4} A_\alpha^i \exp(ik_i z)$. The four coefficients are determined by the boundary conditions that both spinor components are zero at the two film interfaces. This leads to the following equations:

$$\tan\left(k_1 \frac{k_0 t}{2}\right) = \frac{k_2}{\sqrt{k_2^2+\eta^2} \pm \eta} \frac{\sqrt{k_1^2+\eta^2} \pm \eta}{k_1} \tan\left(k_2 \frac{k_0 t}{2}\right) \tag{3}$$

where $\eta = m_l|\delta|/(\hbar k_0)^2$. The value of

$$k_2 = \sqrt{k_1^2 + 4 - 4\sqrt{k_1^2+\eta^2}} \tag{4}$$

becomes imaginary at high η values. Then the trigonometric functions in (3) are replaced by the hyperbolic ones. Special care must be taken to choose the correct branch of $\sqrt{k_2^2+\eta^2}$ in (4): the sign of $\sqrt{k_2^2+\eta^2}$ must be alternated after the argument becomes zero.

For arbitrary parameters, (3) has to be solved numerically. We present results of the numerical solution in the next section. However, to gain an insight into the results, it is sufficient to analyze the solutions in case of small strain.

Introducing $y_n = (k_1 - k_2)/2$, (3) can be written in the following form [19]:

$$\sin(y_n k_0 t) = \pm \frac{\eta y_n \sin(\sqrt{((1-\eta^2-y_n^2)/(1-y_n^2))}k_0 t)}{\sqrt{(1-y_n^2)(1-\eta^2-y_n^2)}}. \tag{5}$$

Solving (5) by perturbations for small values of the parameter η, we obtain the following dispersion relation for the unprimed subbands n:

$$E_n^{\pm} = \frac{\hbar^2}{2m_l}\left(\frac{\pi n}{t}\right)^2 + \hbar^2 \frac{k_x^2+k_y^2}{2m_t} \pm \left(\frac{\pi n}{k_0 t}\right)^2 \frac{|D\varepsilon_{xy} - (\hbar^2 k_x k_y/M)|}{k_0 t|1-(\pi n/k_0 t)^2|} \sin(k_0 t). \tag{6}$$

Equation (6) demonstrates that the unprimed subbands are not necessarily degenerate and degeneracy is preserved only, when shear strain is zero and either $k_x = 0$ or $k_y = 0$.

B. Valley Splitting in a Magnetic Field

For zero shear strain, the Landau levels in an orthogonal magnetic field B are found from (6) by using the Bohr–Sommerfeld quantization conditions

$$E_m^{(1,2)} = \hbar\omega_c \left(m + \frac{1}{2}\right) \frac{\pi}{4\arctan\left(\sqrt{m_{(1,2)}/m_{(2,1)}}\right)} \tag{7}$$

where

$$m_{(1,2)} = \left(\frac{1}{m_t} \pm \frac{1}{M}\left(\frac{\pi n}{k_0 t}\right)^2 \frac{\sin(k_o t)}{k_0 t|1-(\pi n/k_0 t)^2|}\right)^{-1} \tag{8}$$

and

$$\omega_c = \frac{eB}{\sqrt{m_1 m_2}c}$$

is the cyclotron frequency, e is the electron charge, and c is the speed of light. According to (7), the difference $|E_m^1 - E_m^2|$ is linear regarding the magnetic field.

In Shubnikov-de-Haas experiments, now there will occur two sets of resistance oscillations with slightly different periods in inverse magnetic field resolved. Because of the small difference between the masses, the difference in periods will also be small. However, at the Fermi level, the quantum number *m,* which is proportional to the ratio of the Fermi energy to the cyclotron frequency, is typically very large and may lead to a splitting

of several hundreds microelectronvolts. The difference in the periods can be interpreted as an appearance of an additional energy shift between the equivalent unprimed valleys. Most importantly, the shift is linear in the magnetic field. The linear dependence of splitting between the valleys on the magnetic field will be also observed even in the presence of a small intrinsic constant valley splitting as long as this splitting is much smaller than the Fermi energy. This splitting is possible due to a remaining shear strain and/or conduction band nonparabolicity, which is not accounted for in the two-band $\mathbf{k}\cdot\mathbf{p}$ theory and is usually several tens of microelectronvolts, thus much smaller than the Fermi energy. For a 10-nm-thick silicon film grown on SiGe, it follows from (7) and (8) that the valley splitting can be several tens of microelectronvolts in a magnetic field of 1 T, which is consistent with the experimental observations [7].

C. Valley Splitting in a Point Contact

We consider a point contact in [1 1 0] direction realized by confining an electron system of a thin silicon film laterally by depleting the area under additional gates. Without strain, the low-energy effective Hamiltonian in the point contact can be written as

$$H_{(1,2)} = \frac{\hbar^2 k_x'^2}{2m_{(2,1)}} + \frac{\hbar^2 k_y'^2}{2m_{(1,2)}} + \frac{1}{2}\kappa x'^2 + V_b \qquad (9)$$

where the primed variables are along the [1 1 0] and [1 –1 0] axes, the effective masses are determined by (8), κ is the spring constant of the point contact confinement potential $V(x') = \kappa x'^2/2$ in [1 –1 0] direction, and V_b is a gate–voltage-dependent conduction-band shift in the point contact [20]. The dispersion relation of propagating modes within the point contact is written as

$$E_p^{(1,2)} = \frac{k^2 k_x'^2}{2m_{(2,1)}} + \hbar\omega_{(1,2)}\left(p + \frac{1}{2}\right) + V_b \qquad (10)$$

where $\omega_{(1,2)}^2 = \kappa/m_{(1,2)}$. Since the energy minima of the two propagating modes with the same p are separated, they are resolved in the conductance experiment through the point contact as two distinct steps. The valley splitting is given by $\Delta E_p = \hbar|\omega_1 - \omega_2|$. The difference in the effective masses (8) and, correspondingly, the valley splitting can be greatly enhanced by reducing the effective thickness t of the quasi-2-D electron gas, which is usually the case in a gated electron system, when the inversion layer is formed.

In a [1 0 0] oriented point contact without strain, the effective Hamiltonian is

$$H^{\pm} = \hbar^2\frac{k_x^2 + k_y^2}{2m_t} \pm \left(\frac{\pi n}{k_0 t}\right)^2 \frac{|\hbar^2 k_x k_y/M|\sin(k_o t)}{k_0 t|1 - (\pi n/k_0 t)^2|} + \frac{\kappa}{2}x^2.$$

Due to symmetry with respect to k_y, the subband minima in a point contact are always degenerate. For this reason, the valley splitting in [1 0 0] oriented point contacts is greatly reduced.

D. Valley Splitting by Shear Strain

It follows from (6) that shear strain induces a valley splitting linear in strain for small shear strain values [19]

$$\Delta E_n = 2\left(\frac{\pi n}{k_0 t}\right)^2 \frac{D\varepsilon_{xy}}{k_0 t|1 - (\pi n/k_0 t)^2|}\sin(k_0 t).$$

The subband splitting is inversely proportional to the film thickness in the third power, and thus, can be large in thin films.

One can also evaluate the maximum subband splitting achieved in the limit $\eta \to \infty$. In this limit, it follows from (2) that the band dispersion becomes parabolic again around the minimum located exactly at the X point. The subband quantization energies are thus determined by the usual quantization conditions, which results in the subband splitting

$$\Delta E_n = \left(\frac{\hbar\pi}{t}\right)^2 \frac{2n-1}{2m_t}.$$

For practically relevant intermediate strain values, a numerical solution of (3) is required.

IV. Numerical Results

A. Unprimed Subbands

In order to analyze the subband structure in (0 0 1) oriented thin silicon films, we first approximate the film potential by the square-well potential with infinite potential walls. Although not exact, this is a good approximation for thin films. To obtain the values for the subband splitting and effective masses for an arbitrary strain value, (3) can be solved numerically. Alternatively, the eigenvalues can be found by resolving the equations obtained by discretizing the Hamiltonian (1) with $k_z = -i\frac{d}{dz}$ and the confinement potential $IU(z)$ added. The latter method is more general, because it allows the inclusion of a confinement potential of arbitrary form making self-consistent calculations possible.

Both numerical routines were implemented, and equivalent results were obtained by the two methods in case of a square-well potential with infinite walls.

The splitting between the unprimed subbands with the same quantum number n normalized to the ground subband energy in unstrained films for a film of thickness $t = 6.5$ nm is shown in Fig. 3 as function of shear strain. The dependence is not monotonic and strongly depends on the subband number. Even for the ground subbands with $n = 1$, the splitting is comparable to the subband energy at large strain values. The subband splitting increases rapidly with the film thickness decreased, as demonstrated in Fig. 4. For ultrathin body films, the splitting can reach a value comparable to $k_B T$ already at moderate strain values.

Results shown in Fig. 4 demonstrate that valley splitting can be effectively controlled by adjusting the shear strain and modifying the effective thickness t of the electron system. Uniaxial stress along [1 1 0] channel direction, which induces shear strain, is already used by industry to enhance the performance of MOSFETs. Therefore, its application to control valley splitting does not require expensive technological modifications.

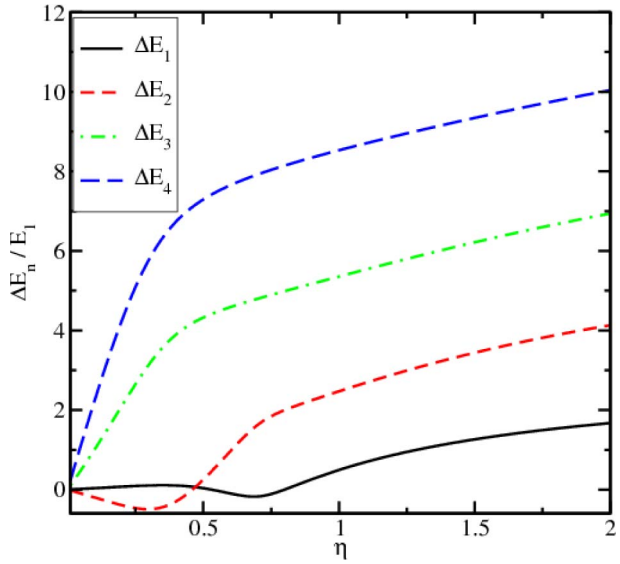

Fig. 3. Splitting between the unprimed subband energies, or the valley splitting, in a 6.5-nm-thick silicon film as a function of shear strain. The splitting values are normalized to the energy of the ground subband without strain. The value $\eta = 1$ corresponds to the shear strain value $\varepsilon_{xy} = 0.016$. The value of valley splitting may alternate its sign, in accordance to (6).

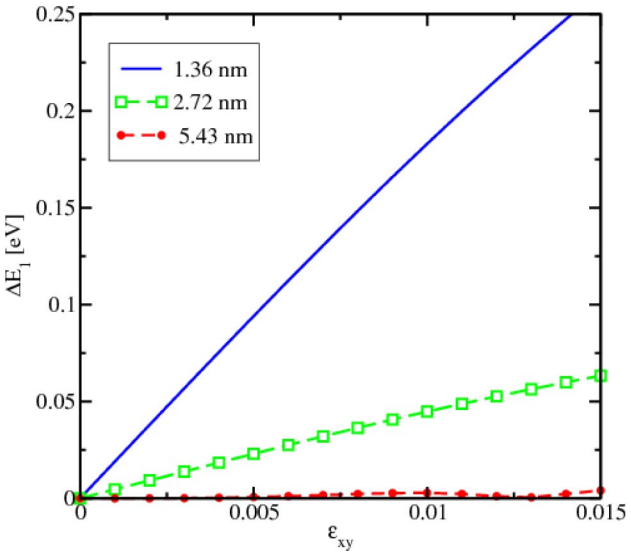

Fig. 4. Shear-strain-induced splitting of the ground subbands for several film thicknesses. In ultrathin films, the splitting is larger than kT already for moderate stress.

The dependence of the subband effective masses in [1 1 0] and [1 –1 0] directions on tensile strain along [1 1 0] direction is shown in Fig. 5. Similar to the bulk results [10], the effective mass decreases in the tensile strain direction along [1 1 0] guaranteeing enhancement of current and mobility by shear strain in thin films. However, the effective masses of the two unprimed subbands with the same quantum number are not equal in thin films even without strain. Fig. 6 demonstrates a strong dependence of the effective masses of the two ground subbands on the film thickness t, also predicted by (8). Subbands are, however, nonparabolic, as shown in the inset of Fig. 6, where the equipotentials of the corresponding dispersion relations for a

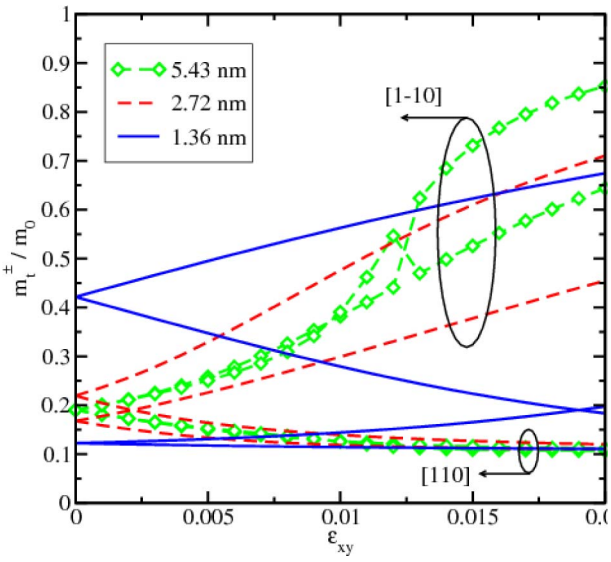

Fig. 5. Effective masses of the two ground subbands. In ultrathin films, the effective masses of the two ground subbands are different even without stress.

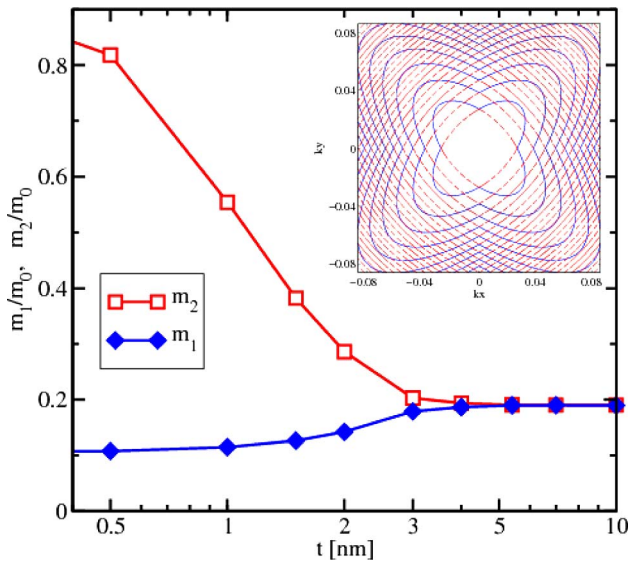

Fig. 6. Thickness dependence in unstrained films of the two lowest unprimed subbands. Inset: contour plots of the two lowest unprimed subbands.

$t = 1.36$ nm thin film are shown. This difference in shape is responsible for the splitting proportional to the strength of an orthogonal magnetic field. The difference in the in-plane masses also guarantees a large subband splitting in [1 1 0] oriented point contacts (10).

B. Primed Subbands

Recent calculations of the primed subbands based on the "linear combination of bulk bands" method obtained with the empirical pseudopotential calculations [21] reveal the dependence of the transport effective masses on silicon film thickness t. Here, we briefly analyze the effective mass of the primed subbands based on the two-band Hamiltonian (1). We assume the quantization direction along the [1 0 0] axis. By formally

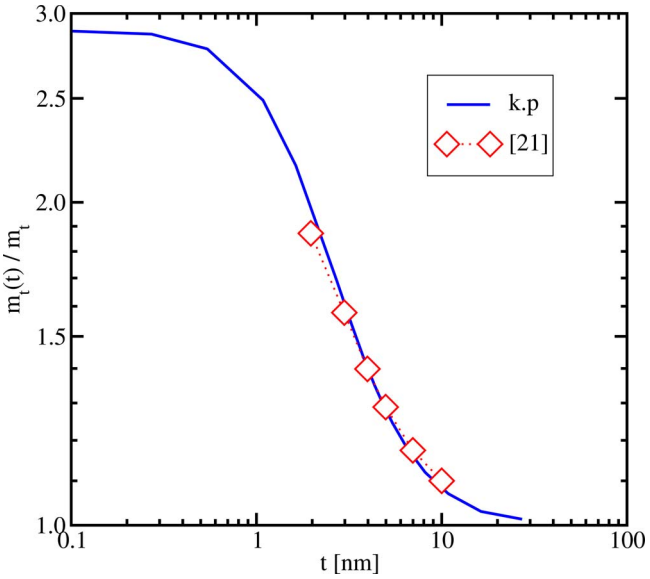

Fig. 7. Thickness dependence of the effective mass of the lowest primed subbands computed with the two-band $\mathbf{k}\cdot\mathbf{p}$ model (solid line) is in excellent agreement with the full-band calculations [21].

replacing k_0/m_l with k_y/M and $k_x\ k_y\ /M$ with $k_z\ k_0/m_l$ in (1) one finds the dispersion relation and the effective masses in the primed subbands, where results of calculations are shown in Fig. 7. The two-band $\mathbf{k}\cdot\mathbf{p}$ results are in excellent agreement with the "linear combination of the bulk bands" method with a potential barrier of 3 eV at the film interface [21].

V. Conclusion

The unprimed valley structure in (0 0 1) thin silicon films has been analyzed with the two-band $\mathbf{k}\cdot\mathbf{p}$ model. It is shown that the twofold degeneracy of the unprimed subbands can be lifted leading to the so-called valley splitting. For the first time, the model predicts that the splitting is proportional to the strength of the perpendicular magnetic field. The valley splitting is significantly enhanced in $\langle 1\,1\,0\rangle$ oriented point contacts, while it should be suppressed in a $\langle 1\,0\,0\rangle$ point contact. Finally, the valley splitting can be controlled and made larger than the Zeeman splitting by shear strain. This makes silicon very attractive for spintronic applications.

Acknowledgment

The authors thank Franz Schanovsky for providing the DFT data.

References

[1] S. Natarajan, M. Armstrong, M. Bost, R. Brain, M. Brazier, C.-H. Chang, V. Chikarmane, M. Childs, H. Deshpande, K. Dev, G. Ding, T. Ghani, O. Golonzka, W. Han, J. He, R. Heussner, R. James, I. Jin, C. Kenyon, S. Klopcic, S.-H. Lee, M. Liu, S. Lodha, B. McFadden, A. Murthy, L. Neiberg, J. Neirynck, P. Packan, S. Pae, C. Parker, C. Pelto, L. Pipes, J. Sebastian, J. Seiple, B. Sell, S. Sivakumar, B. Song, K. Tone, T. Troeger, C. Weber, M. Yang, A. Yeoh, and K. Zhang, "A 32 nm logic technology featuring 2 nd-generation high-k + metal-gate transistors, enhanced channel strain and 0.171 μm^2 SRAM cell size in a 291 Mb array," in *IEDM Tech. Dig.*, 2008, pp. 941–943.

[2] P. Packan, S. Akbar, M. Armstrong, D. Bergstrom, M. Brazier, H. Deshpande, K. Dev, G. Ding, T. Ghani, O. Golonzka, W. Han, J. He, R. Heussner, R. James, J. Jopling, C. Kenyon, S.-H. Lee, M. Liu, S. Lodha, B. Mattis, A. Murthy, L. Neiberg, J. Neirynck, S. Pae, C. Parker, L. Pipes, J. Sebastian, J. Seiple, B. Sell, A. Sharma, S. Sivakumar, B. Song, A. St. Amour, K. Tone, T. Troeger, C. Weber, K. Zhang, Y. Luo, and S. Natarajan, "High performance 32 nm logic technology featuring 2 nd generation high-k + metal gate transistors," in *IEDM Tech. Dig.*, 2009, pp. 1–4.

[3] M. Radosavljevic, B. Chu-Kung, S. Corcoran, G. Dewey, M.K. Hudait, J.M. Fastenau, J. Kavalieros, W.K. Liu, D. Lubyshev, M. Metz, K. Millard, N. Mukherjee, W. Rachmady, U. Shah, and R. Chau, "Advanced high-k gate dielectric for high-performance short-channel $In_{0.7}Ga_{0.3}As$ quantum well field effect transistors on silicon substrate for low power logic applications," in *IEDM Tech. Dig.*, 2009, pp. 1–4.

[4] R. Chau, "Challenges and opportunities of emerging nanotechnology for future VLSI nanoelectronics," presented at the Rec. Int. Semicond. Device Res. Symp. (ISDRS), College Park, MD, 2007, p. 3.

[5] S. S. P. Parkin, M. Hayashi, and L. Thomas, "Magnetic domain-wall racetrack memory," *Science*, vol. 320, no. 5873, pp. 190–194, 2008.

[6] I. Appelbaum, B. Huang, and D. J. Monsma, "Electronic measurement and control of spin transport in silicon," *Nature*, vol. 447, no. 7142, pp. 295–298, 2007.

[7] S. Goswami, K. A. Slinker, M. Friesen, L. M. McGuire, J. L. Truitt, C. Tahan, L. J. Klein, J. O. Chu, P. M. Mooney, D. W. van der Weide, R. Joynt, S. N. Coppersmith, and M. A. Eriksson, "Controllable valley splitting in silicon quantum devices," *Nature Phys.*, vol. 31, no. 1, pp. 41–45, 2007.

[8] G. L. Bir and G. E. Pikus, *Symmetry and Strain-Induced Effects in Semiconductors*. New York: Wiley, 1974.

[9] J. C. Hensel, H. Hasegawa, and M. Nakayama, "Cyclotron resonance in uniaxially stressed silicon. II. Nature of the covalent bond," *Phys. Rev*, vol. 138, no. 1A, pp. A225–A238, 1965.

[10] E. Ungersböck, S. Dhar, G. Karlowatz, V. Sverdlov, H. Kosina, and S. Selberherr, "The effect of general strain on band structure and electron mobility of silicon," *IEEE Trans. Electron Devices*, vol. 54, no. 9, pp. 2183–2190, Sep. 2007.

[11] G. Kresse and J. Hafner, "Ab initio molecular dynamics for liquid metals," *Phys. Rev. B*, vol. 47, no. 1, pp. 558–561, 1993.

[12] G. Kresse and J. Hafner, "Ab initio molecular-dynamics simulation of the liquid-metal-amorphous-semiconductor transition in germanium," *Phys. Rev. B*, vol. 49, no. 20, pp. 14251–14269, 1994.

[13] G. Kresse and J. Furthmüller, "Efficient iterative schemes for ab initio total-energy calculations using a plane-wave basis set," *Phys. Rev. B*, vol. 54, no. 16, pp. 11169–11186, 1996.

[14] G. Kresse and J. Furthmüller, "Efficiency of ab-initio total energy calculations for metals and semiconductors using a plane-wave basis set," *Comput. Mat. Sci.*, vol. 6, no. 1, pp. 15–50, 1996.

[15] T. B. Boykin, G. Klimeck, and F. Oyafuso, "Valence band effective-mass expressions in the sp^3d^5 s^* empirical tight-binding model applied to a Si and Ge parametrization," *Phys. Rev. B*, vol. 69, no. 11, pp. 115201-1–115201-10, 2004.

[16] V. Sverdlov, G. Karlowatz, S. Dhar, H. Kosina, and S. Selberherr, "Two-band k.p model for the conduction band in silicon: Impact of strain and confinement on band structure and mobility," *Solid-State Electron*, vol. 52, no. 10, pp. 1563–1568, 2008.

[17] M. Friessen, S. Chutia, C. Tahan, and S. N. Coppersmith, "Valley splitting theory of SiGe/Si/SiGe quantum wells," *Phys. Rev. B*, vol. 75, no. 11, pp. 115318-1–115318-12, 2007.

[18] O. Baumgartner, M. Karner, V. Sverdlov, and H. Kosina, "Numerical quadrature of the subband distribution functions in strained silicon UTB devices," in *Proc. 13th Int. Workshop Comput. Electron.*, 2009, pp. 53–56.

[19] V. Sverdlov and S. Selberherr, "Electron subband structure and controlled valley splitting in silicon thin-body SOI FETs: Two-band k.p theory and beyond," *Solid-State Electron*, vol. 52, no. 12, pp. 1861–1866, 2008.

[20] B. van Wees, H. van Houten, and C. Beenakker, "Quantized conductance of point contacts in a two-dimensional electron gas," *Phys. Rev. Lett.*, vol. 60, no. 9, pp. 848–850, 1988.

[21] J. Van Der Steen, D. Esseni, P. Palestri, L. Selmi, and R. J. E. Hueting, "Validity of the parabolic effective mass approximation in silicon and germanium n-MOSFETs with different crystal orientations," *IEEE Trans. Electron. Devices*, vol. 54, no. 8, pp. 1843–1851, Aug. 2007.

Oskar Baumgartner was born in Krems an der Donau, Austria, in 1982. He received the Dipl.Ing. degree in electrical engineering in January 2007 from the Technische Universität Wien, Wien, Austria, where he is currently working toward the Ph.D. degree at the Institute for Microelectronics.

His current research interests include the modeling and simulation of quantum transport in optical and nanoelectronic devices.

Viktor Sverdlov received the M.Sc. and Ph.D. degrees in physics from the State University of St.Petersburg, St. Petersburg, Russia, in 1985 and 1989, respectively.

From 1989 to 1999, he was a Staff Research Scientist at the V. A. Fock Institute of Physics, State University of St. Petersburg. During this time, he visited Abdus Salam International Centre for Theoretical Physics (Italy, 1993), the University of Geneva (Switzerland, 1993–1994), the University of Oulu (Finland, 1995), the Helsinki University of Technology (Finland, 1996, 1998), the Free University of Berlin (Germany, 1997), and NORDITA (Denmark, 1998). In 1999, he became a Staff Research Scientist at the State University of New York at Stony Brook. He joined the Institute for Microelectronics, Technische Universität Wien, Wien, Austria, in 2004. His current research interests include device simulations, computational physics, solid-state physics, and nanoelectronics.

Thomas Windbacher was born in Mödling, Austria, in 1979. He received the Dipl.Ing. degree in physics in October 2006 from the Technische Universität Wien, where he is currently working toward the Ph.D. degree from the Institute for Microelectronics.

His current research interests include modeling and simulation of dopant diffusion (transient-enhanced diffusion).

Siegfried Selberherr (F'93) was born in Klosterneuburg, Austria, in 1955. He received the Dipl.Ing. degree in electrical engineering and the Ph.D. degree in technical sciences from the Technische Universität Wien, Wien, Austria, in 1978 and 1981, respectively.

He has been holding the *venia docendi* on computer-aided design since 1984. Since 1988, he has been the Chair Professor of the Institute for Microelectronics, Technische Universität Wien. From 1998 to 2005, he was the Dean of the Fakultät für Elektrotechnik und Informationstechnik. His current research interests include modeling and simulation of problems for microelectronics engineering.